ORGANOMETALLICS

pubs.acs.org/Organometallics Article

Lithium Hexaphenylrhodate(III) and -Iridate(III): Structure in the Solid State and in Solution

Takanori Iwasaki,* Yuko Hirooka, Hikaru Takaya, Tetsuo Honma, and Kyoko Nozaki*

Cite This: *Organometallics* 2021, 40, 2489−2495 Read Online

ACCESS | Metrics & More | Article Recommendations | Supporting Information

ABSTRACT: Anionic homoleptic organo−transition metal complexes can be prepared from organolithium reagents and transition metal salts and are key reactive intermediates in C−C bond formation. However, the interaction between the anionic component and cationic counterparts of multianionic homoleptic organo−transition metal complexes in solution remains unclear, unlike well-studied monoanionic complexes such as organocuprates. Here we have prepared and structurally characterized lithium hexaphenylrhodate(III) and -iridate(III) complexes, $[Li(12\text{-crown-}4)_2][MPh_6\{Li(thf)\}_2]$ (M = Rh and Ir), as the first examples of hexaaryl complexes of d^6 metals. In the crystals, two Li cations contact the trianionic MPh_6 moiety, while the other exists as a solvent-separated ion pair. In THF, hexaphenylrhodate decomposed within 1 h. In contrast, the Ir analog was stable. ^{7}Li NMR and X-ray absorption fine structure analysis revealed the solution-phase structure of hexaphenyliridate, which maintained a partially contacted ion pair structure even in THF, a coordinating solvent.

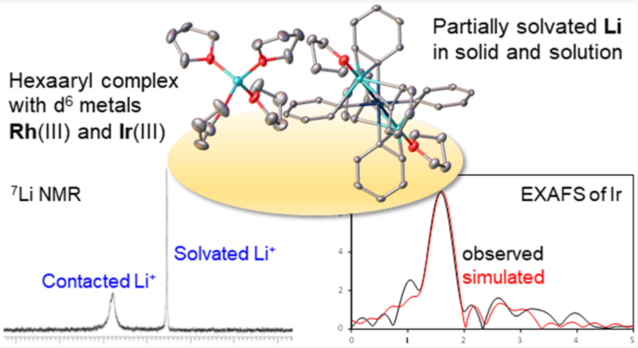

■ INTRODUCTION

Homoleptic organo−transition metal complexes consisting of a transition metal center and identical carbanion moieties are produced by reacting transition metal salts with organometallic reagents and have gained attention because of their unique reactivities[1] and structural features.[2] Since homoleptic organo−transition metal complexes carry carbanions as the sole ligands, they often have a formal anionic charge(s) on the transition metal center; thus, a countercation(s) such as Li cations will coexist. In the case of the hexamethyl complexes $Li^+_n[MMe_6]^{n-}$ (Figure 1A), all Li cations contact their anionic counterpart by the $Li\cdots CH_3$ interaction.[3] Similarly, the hexaalkynyl complexes $Li^+_n[M(CCR)_6]^{n-}$ (Figure 1B) form a contact ion pair (CIP) by cation−π interactions.[4] In contrast, hexaaryl complexes form not only a CIP (Figure 1C) but also a solvent-separated ion pair (SSIP) (Figure 1D) in the solid state.[5−7] For instance, all the Li cations in $Li^+_3[CrPh_6]^{3-}$ and $Li^+_4[VPh_6]^{4-}$ contact their anionic counterparts,[7] but the Li cations in the Zr(IV), Hf(IV), and Nb(IV) analogs exist as SSIPs in the solid state.[5] Interestingly, in these examples, all the Li cations are either solvated or contact their anionic counterparts except for polymorphic $Li^+_2[HfPh_6]^{2-}$.[8] The existence of these interactions between anionic components and cationic counterparts has only been discussed based on crystal structures. In contrast to the well-understood cation−anion interactions of monoanionic transition metal complexes,[9] particularly those of cuprates,[10] the solution-phase structure of these multianionic homoleptic organo−transition metal complexes has never been addressed. Therefore, the interaction between multianionic organo−transition metal species and their counter cations remains a significant knowledge gap compared with monoanionic species.

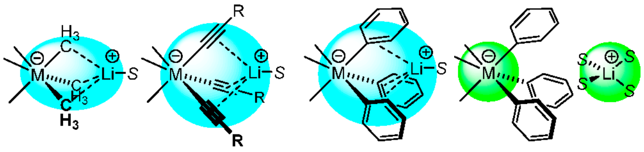

A: $Li^+_n[MMe_6]^{n-}$ **B:** $Li^+_n[M(C{\equiv}CR)_6]^{n-}$ **C:** *CIP*-$Li^+_n[MPh_6]^{n-}$ **D:** *SSIP*-$Li^+_n[MPh_6]^{n-}$

Figure 1. Schematic drawing of the molecular structure of homoleptic hexamethyl, hexaalkynyl, and hexaaryl complexes. M: transition metal, S: solvent.

Here we report the synthesis of novel lithium hexaarylrhodate(III) and -iridate(III) complexes, $Li^+_3[MPh_6]^{3-}$ (M = Rh and Ir), and their molecular structures in the solid state and in solution. Structural analyses revealed

Received: April 23, 2021
Published: July 23, 2021

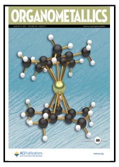

ACS Publications

https://doi.org/10.1021/acs.organomet.1c00248
Organometallics 2021, 40, 2489−2495

that two Li cations contact the anionic hexaphenylmetalate moiety, while the other coexists as an SSIP in the solid state. The interaction between the two Li cations and the anionic component is maintained even in a coordinating solvent.

■ RESULTS AND DISCUSSION

Treatment of *mer*-$RhCl_3(tht)_3$ complex $\mathbf{1_{Rh}}$ (tht = tetrahydrothiophene) with 8 equiv of PhLi in THF followed by the addition of hexane afforded $\mathbf{2_{Rh}}$ as a beige precipitate in 70% yield. NMR analysis of obtained compound $\mathbf{2_{Rh}}$ showed only one set of Ph groups. Iridium analog $\mathbf{2_{Ir}}$ was successfully obtained in 76% yield as a white solid from corresponding Ir complex $\mathbf{1_{Ir}}$ (Scheme 1).

Scheme 1. Synthesis of Rhodate $\mathbf{2_{Rh}}$ and Iridate $\mathbf{2_{Ir}}$

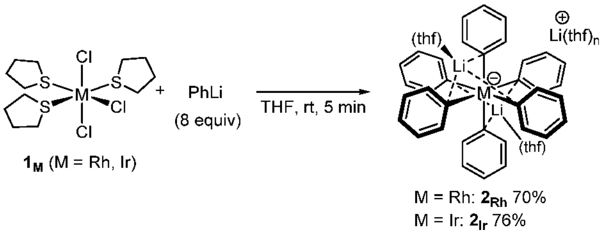

Isolated $\mathbf{2_{Rh}}$ was unstable in THF and fully decomposed within 60 min at 21 °C (Figure S8).[11] The decomposition process obeys second-order kinetics with respect to $\mathbf{2_{Rh}}$ (Figure S9). These results suggest that the observed decomposition involves the disproportionation of $\mathbf{2_{Rh}}$, such as two Rh(III) to one Rh(II) and Rh(IV) species, and the reductive elimination of biphenyl from these paramagnetic species. In contrast, $\mathbf{2_{Ir}}$ did not decompose in THF at ambient temperature at least for several days.

The reaction of $\mathbf{1_{Ir}}$ with 3 equiv of PhLi in THF/THF-d_8 reached completion within 10 min to afford a mixture of $\mathbf{1_{Ir}}$ and $\mathbf{2_{Ir}}$ in an approximately 6:4 ratio without other intermediates bearing five or fewer Ph moieties. Further addition of 3 equiv of PhLi (6 equiv in total) afforded $\mathbf{2_{Ir}}$ in 77% yield as the sole product (Scheme 2, Figure S10). These results could be explained by assuming a dissociative mechanism wherein THT dissociates from the Ir center and one Ph group binds to Ir. Once a Ph group binds to the Ir center, ligand exchange between the THT/Cl moieties and PhLi is accelerated by the stronger *trans*-effect of the Ph moiety. Therefore, intermediates bearing five or fewer Ph moieties were not observed.

Scheme 2. Stoichiometric Reaction of $\mathbf{1_{Ir}}$ with PhLi

$$\mathbf{1_{Ir}} \xrightarrow[\text{THF/THF-}d_8\text{, rt}]{\text{PhLi (3 equiv)}} \underset{58\%}{\mathbf{1_{Ir}}} + \underset{41\%}{\mathbf{2_{Ir}}} \xrightarrow[\text{THF/THF-}d_8\text{, rt}]{\text{PhLi (3 equiv)}} \underset{77\%}{\mathbf{2_{Ir}}}$$

Organomagnesium reagents are often used to synthesize anionic organo−transition metal species. Indeed, we have reported that both organolithium and -magnesium reagents yield the same monoanionic organometalates,[12,13] but this is not the case. The use of PhMgBr instead of PhLi resulted in the formation of a different species than in the reaction of $\mathbf{1_{Ir}}$ with PhLi, though the actual structure could not been determined.

The molecular structures of hexaphenylmetalates $\mathbf{3_{Rh}}$ and $\mathbf{3_{Ir}}$ were unambiguously determined by X-ray diffraction analysis (Figure 2). Single crystals of $\mathbf{3_{Rh}}$ and $\mathbf{3_{Ir}}$ suitable for X-ray crystallography were obtained by recrystallization of $\mathbf{2_{Rh}}$ and $\mathbf{2_{Ir}}$ from THF and pentane in the presence of 12-crown-4, respectively. The crystal structure of $\mathbf{3_{Rh}}$ contains one Rh bearing six Ph moieties in an ideal octahedral geometry and three Li cations. Two Li cations with one THF molecule contact the Ph moieties on Rh, and the other in the outer sphere is surrounded by two 12-crown-4 molecules. The molecular structure of $\mathbf{3_{Ir}}$ was nearly identical to that of $\mathbf{3_{Rh}}$. When $\mathbf{2_{Ir}}$ was recrystallized from THF in the absence of 12-

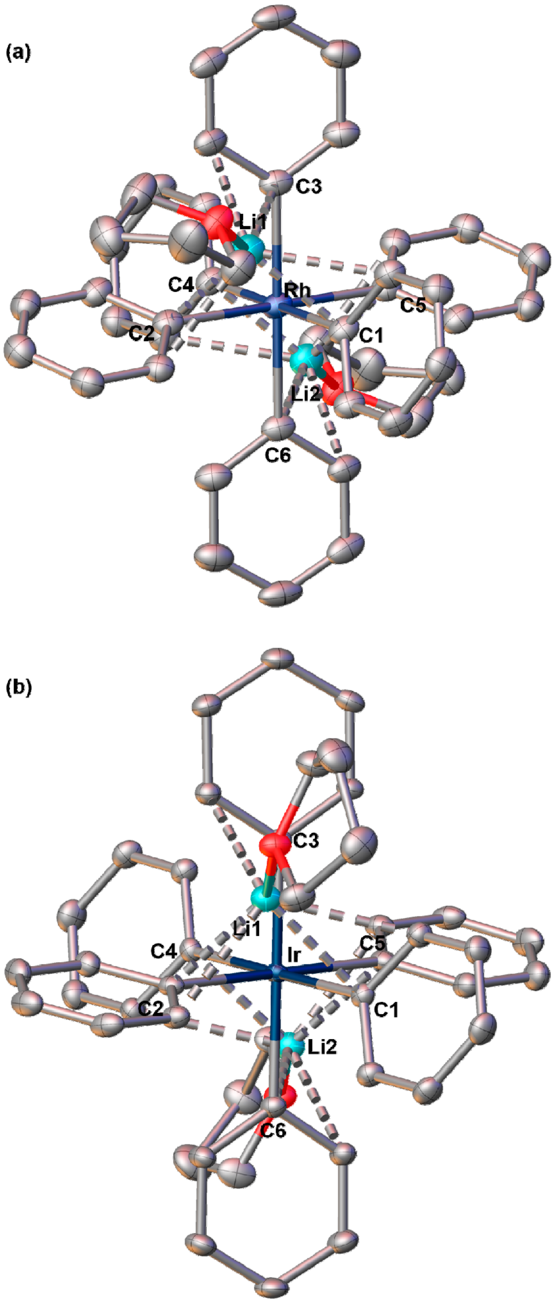

Figure 2. ORTEP drawing of anionic part of (a) [Li(12-crown-4)$_2$][RhPh$_6${Li(thf)}$_2$] ($\mathbf{3_{Rh}}$) and (b) [Li(12-crown-4)$_2$][IrPh$_6${Li-(thf)}$_2$] ($\mathbf{3_{Ir}}$) with thermal ellipsoids at the 50% probability level. Deep blue: Rh and Ir, light blue: Li, gray: C, and red: O. Counter cation [Li(12-crown-4)$_2$], all hydrogen atoms, noncoordinating solvent molecules, and disordered molecules are omitted for clarity.

crown-4, a similar molecular structure $\mathbf{2_{Ir}}$ containing the $IrPh_6$ anion with two contacted Li cations and one THF-solvated Li cation was also obtained (Figure S11).

Despite satisfying the 18-electron rule, hexaaryl d^6 metal complexes have never been reported. Attempts to synthesize aryl complexes of Rh(III) using pentachlorophenyl and pentafluorophenyl lithium reagents[14] led to the formation of tetraarylrhodate(II) ($[Rh(II)(C_6Cl_5)_4]^{2-}$)[15] and pentaarylrhodate(III) ($[Rh(III)(C_6F_5)_5]^{2-}$),[16] respectively. In addition, tetraarylcobalate(III)[17] and tetraarylferrate(II)[18] complexes have also been reported. Only sterically less congested hexamethyl[3e−i] and hexaalkynyl,[4e4i] d^6 metal complexes have been reported. The difficulty in producing hexaaryl d^6 metal complexes is partly due to the shorter covalent radii of d^6 late transition metals compared with those of d^0 and d^3 metals (*vide infra*).[19] The key to the successful synthesis of the novel hexaaryl d^6 metal complexes is stabilization of the Rh^{3-} and Ir^{3-} centers by the interaction of the Ir−C σ-bond[20] and the π-bonding electrons of the phenyl moieties[21,22] with Li cations. This interaction delocalizes the negative formal charge on the anionic Rh and Ir centers to the two Li cations to stabilize the higher anionic state.

The selected bond lengths and angles of $\mathbf{3_{Rh}}$ and $\mathbf{3_{Ir}}$ are summarized in Table 1. The crystal structure of $\mathbf{3_{Rh}}$ has inversion symmetry at the Rh center. The Rh−C bond lengths of $\mathbf{3_{Rh}}$ are in the range of 2.148−2.152 Å, and the *cis*-oriented C−Rh−C angles are in the range of 87.2−92.8°. Because two Li cations contact each relative corner of the octahedral structure, the C−Rh−C angles of the lithium-contacted corners (e.g., C1−Rh−C2) are slightly wider than the others (e.g., C2−Rh−C4). The bond lengths and angles of the crystal structure of $\mathbf{3_{Ir}}$ are almost the same as those of $\mathbf{3_{Rh}}$ (the average C−Rh bond lengths in $\mathbf{3_{Rh}}$ and C−Ir bond lengths in $\mathbf{3_{Ir}}$ are both 2.150 Å).

Table 1. Selected Bond Lengths (Å) and Angles (deg) of $\mathbf{3_{Rh}}$ and $\mathbf{3_{Ir}}$[a]

	$[Li(12\text{-crown-}4)_2]$ $[RhPh_6\{Li(thf)\}_2]$ ($\mathbf{3_{Rh}}$)	$[Li(12\text{-crown-}4)_2]$ $[IrPh_6\{Li(thf)\}_2]$ ($\mathbf{3_{Ir}}$)
M−C1	2.148(4)	2.151(2)
M−C2	2.152(4)	2.152(2)
M−C3	2.151(4)	2.154(2)
M−C4	2.148(4)	2.148(2)
M−C5	2.152(4)	2.148(2)
M−C6	2.151(4)	2.147(2)
M−Li1	2.546(7)	2.569(5)
M−Li2	2.546(7)	2.587(5)
C1−M−C2	92.76(14)	91.49(9)
C2−M−C3	91.63(14)	91.84(9)
C3−M−C1	91.18(14)	92.72(9)
C2−M−C4	87.24(15)	88.74(9)
C4−M−C3	88.82(14)	86.83(9)
Li1−M−Li2	180.0(2)	179.21(15)

[a] $\mathbf{3_{Rh}}$ has an inversion symmetry at the Rh atom, and thus C4, C5, and C6 correspond to C1*, C2*, and C3*, respectively, by $1 - x$, $1 - y$, and $-z$ symmetric operation.

The average C−M bond lengths in the literature are $[Zr(IV)Ph_6]^{2-}$: 2.362 Å,[5] $[Hf(IV)Ph_6]^{2-}$: 2.378 Å,[5] $[Ta(V)Ph_6]^{-}$: 2.290 Å,[6] $[Nb(IV)Ph_6]^{2-}$: 2.284 Å,[5] $[V(II)Ph_6]^{4-}$: 2.352 Å,[7] and $[Cr(III)Ph_6]^{3-}$: 2.240 Å.[7] The bond length tends to decrease for larger group numbers in the same period. A comparison of the C−M bond lengths of $\mathbf{3_{Rh}}$ and $\mathbf{3_{Ir}}$ with those of these reported hexaphenyl complexes revealed that the present $\mathbf{3_{Rh}}$ and $\mathbf{3_{Ir}}$ have much shorter C−M bonds, which is consistent with their small covalent radii.

To determine whether the partial SSIP structure is maintained in a coordinating solvent or the Li cations become completely solvated to form trianionic hexaphenylrhodate and -iridate ions, we next carried out solution-phase structural analyses. ^{7}Li NMR of $\mathbf{2_{Ir}}$ in THF-d_8 (2.5 mM) at 20 °C showed a broad signal at +0.26 ppm, which became sharp and shifted slightly upfield upon heating to 60 °C. However, cooling the sample to −60 °C split the signal into two at +0.78 and −0.45 ppm in a 2:1 ratio (Figure 3a).[23] The lower-field signal at +0.78 ppm could be assigned to the contacted Li cations, and the signal at −0.45 ppm was assigned to the solvated Li cation.[24] On the basis of variable-temperature (VT) NMR analysis, the contacted Li cations exchange with the solvated Li cation on the NMR time scale. In sharp contrast to facile solvation of Li cation in lithium cuprates by THF,[25] two Li cations in $\mathbf{2_{Ir}}$ maintained the CIP structure even in THF. When a similar NMR analysis was conducted in the presence of 40 equiv of 12-crown-4, the upper-field signal shifted significantly from −0.45 to −1.42 ppm. In contrast, the chemical shift of the lower-field signal was almost the same (+0.77 ppm) (Figure 3b). Furthermore, the addition of 12-crown-4 decelerated the exchange reaction between the contacted Li cations and the solvated one. The fact that 12-crown-4 slowed the Li exchange reaction suggests that the exchange reaction proceeds via an associative mechanism involving the three Li-cation-contacted intermediates.

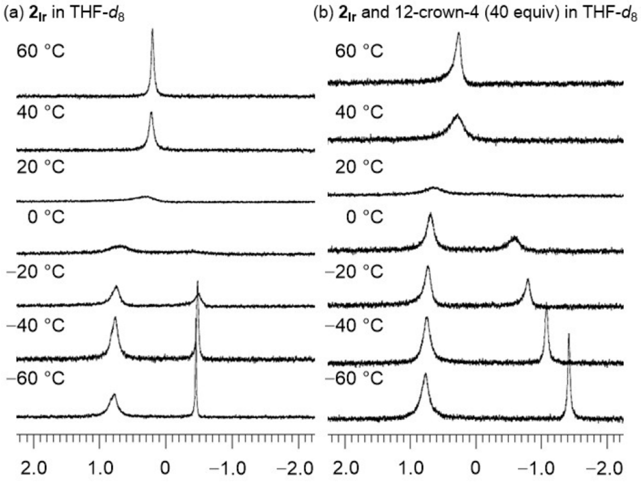

Figure 3. ^{7}Li NMR of (a) $\mathbf{2_{Ir}}$ in THF-d_8 (2.5 mM) and (b) $\mathbf{2_{Ir}}$ and 40 equiv of 12-crown-4 in THF-d_8 (2.5 mM) at various temperature.

The structure of $\mathbf{2_{Ir}}$ was further investigated by solution-phase X-ray absorption fine structure (XAFS) analyses. Figure 4a shows the X-ray absorption near edge structure (XANES) measurements at the Ir L_{III}-edge of $\mathbf{2_{Ir}}$ in THF (red solid line). An intense, sharp white line was observed at 11.223 keV, which corresponds to photoelectron transitions between the Ir $2p_{3/2}$ and upper $5d_{3/2,5/2}$ states. To determine the oxidation state of the Ir center in $\mathbf{2_{Ir}}$, $\mathbf{1_{Ir}}$ (blue dashed line) and IrO_2 (green dashed line) as reference materials containing iridium in oxidation states of +3 and +4, respectively, were also measured. The white-line intensity of the XANES spectrum of $\mathbf{2_{Ir}}$ was

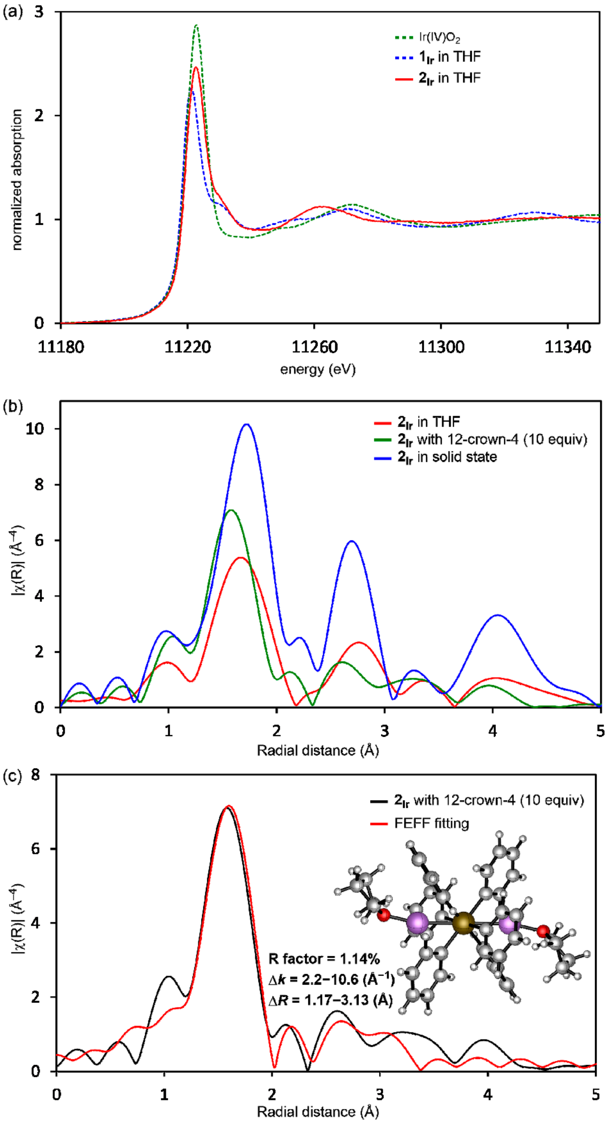

Figure 4. XAFS spectra of 2_{Ir}. (a) XANES spectra of IrO_2 in the solid state (green dashed line), 1_{Ir} in THF (10 mM) (blue dashed line), and 2_{Ir} in THF (1 mM) (red solid line). (b) Radial structure functions of 2_{Ir} (1 mM) (red line) in THF; 2_{Ir} (1 mM) and 10 equiv of 12-crown-4 in THF (green line); and 2_{Ir} in the solid-state (blue line). (c) Radial structure functions of 2_{Ir} (1 mM) and 10 equiv of 12-crown-4 in THF (black line) and the FEFF-simulated fit (red line).

closer to that of 1_{Ir} than that of IrO_2, indicating that the oxidation state of the Ir center in 2_{Ir} is +3.

Figure 4b shows the radial structure functions (RSFs) determined by the extended X-ray absorption fine structure (EXAFS) spectra of 2_{Ir} in the solid state (blue line) and in THF (red and green lines). These spectra exhibit strong peaks at ca. 1.7 and 2.8 Å corresponding to Ir—*ipso*-phenyl-C and Ir—*ortho*-phenyl-C single scatterings and a peak at ca. 4.1 Å corresponding to Ir—phenyl-C multiscattering (see the Supporting Information). The peaks in the solution phase were significantly weaker than those in the solid state because of the fluxionality of phenyl ligands in THF solutions. The addition of 12-crown-4 (10 equiv) to the THF solution led to no significant change (Figure 4b, red and green lines). The similar profiles of RSFs in the solid state or in solution phase indicate that the $IrPh_6$ moiety of 2_{Ir} basically remains in either the solid state or the solution phase (Figure 4b, red and blue lines).

The solution-phase structure of 2_{Ir} was finally confirmed by FEFF-fitting analysis using atomic coordinate extracted from the DFT-optimized structure of $[IrPh_6\{Li(thf)\}_2]^-$ as shown in Figure 4c (see the Supporting Information). The excellent agreement between experimental (Figure 4c, black line) and the FEFF-simulated RSF based on $[IrPh_6\{Li(thf)\}_2]^-$ moiety (Figure 4c, red line) with a good *R* factor (1.14%) adequately supports the contact of two Li cations as exhibited in the single-crystal X-ray structure (Figure 2). These NMR and XAFS analyses clearly showed that the two Li cations contact the $IrPh_6$ moiety even in THF.[25]

Since 2_{Ir} is coordinatively saturated, it should be inert toward electrophiles if the dissociation of PhLi from the Ir center is not allowed. To investigate the dissociation of PhLi from 2_{Ir}, 2_{Ir} was reacted with CO_2 and CO (Scheme 3). When 2_{Ir} was reacted with CO_2 gas (1 atm) in THF-d_8 at room temperature for 24 h, no reaction occurred, and 2_{Ir} remained intact. In addition, CO, which is a good π-accepting ligand and is often used for preparing ate-complexes,[26] did not react with 2_{Ir}. These results imply that the dissociation of PhLi from 2_{Ir} does not proceed at ambient temperatures.

Scheme 3. Reactivity of 2_{Ir} to Small Molecules

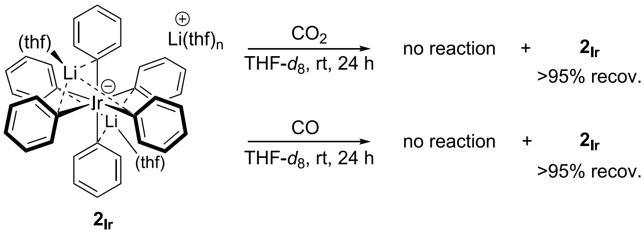

■ CONCLUSION

The interaction between the anionic component and cationic counterparts of multianionic homoleptic organo—transition metal complexes has mainly been discussed based on crystallographic analysis in previous research; thus, the interaction in the solution phase remains unclear. The present study revealed that two of the three coexisting Li cations in the lithium hexaphenylrhodate(III) and -iridate(III) complexes contact the MPh_6 moiety (M = Rh and Ir), while the other exists as an SSIP in the solid state. The partial SSIP structure of $[Li(thf)_4][MPh_6\{Li(thf)\}_2]$ remained even in THF, a coordinating solvent. These results provide important insights for understanding the structure and reactivity of synthetically useful organometalates.

■ EXPERIMENTAL SECTION

General Methods and Materials. Nuclear magnetic resonance spectra were recorded on a Bruker Ascend 500 (^{1}H: 500 MHz, ^{13}C: 126 MHz) spectrometer, a JEOL ECS400 (^{1}H: 400 MHz) spectrometer, or a JEOL ECZ-500R (^{1}H: 500 MHz, ^{7}Li: 194 MHz) spectrometer in 5 mm NMR tubes. All ^{1}H NMR chemical shifts were reported in ppm relative to solvent residual signal of THF-d_7 at δ 3.58. All ^{13}C NMR chemical shifts were reported in ppm relative to carbon resonance in THF-d_8 at δ 67.21 or CD_3CN at δ 118.26. All ^{7}Li NMR chemical shifts were reported in parts per million (ppm) relative to external standard of LiBr in D_2O at δ 0.00. Melting points were measured using Stanford Research Systems OptiMelt MPA 100 with a glass capillary. X-ray crystallography was made on a Rigaku Varimax with HyPix diffractometer using mirror-monochromated Mo Kα radiation (see the Supporting Information for details). Ir L_{III}-edge XANES and EXAFS measurements were carried out at the BL14B2 beamline of the synchrotron SPring-8 in Japan under standard beamline conditions of BL14B2. The Ir L_{III}-edge (11.22 keV) XAFS data were corrected by transmission mode using N_2/Ar mixed gas-filled ionization chambers with the optimized gas ratio and pressure or by fluorescence mode using 19-element Ge solid-state detector (19-SSD) with Si (111) double-crystal monochromator. For the energy calibration of XANES spectra of Ir L_{III}-edge, iridium metal powder was used as a reference sample to set the inflection point determined by the maximum first-derivative of XANES spectra to 11218 eV (see the Supporting Information for details).

All manipulations involving air- and moisture-sensitive compounds were carried out using standard Schlenk techniques under a nitrogen atmosphere or in a glovebox under argon atmosphere. Dehydrated hexane, THF, and Et_2O were purchased from Kanto Chemical Company and purified by SPS[27] prior to use unless otherwise noted. The 12-crown-4 used was dried over Na benzophenone ketyl and distilled under a reduced presser. Other dehydrated solvents were purchased from Wako and used without further purification. *mer*-$RhCl_3(tht)_3$ ($\mathbf{1_{Rh}}$) and *mer*-$IrCl_3(tht)_3$ ($\mathbf{1_{Ir}}$) were synthesized according to the literature.[28] All other commercially available reagents were used as received unless otherwise stated.

Solvent-Free PhLi.[29] In a three-necked flask, phenyl iodide (24.76 g, 0.121 mol) was dissolved in benzene (40 mL). To this mixture, *n*-BuLi (in hexane, 2.67 M, 39.0 mL, 0.104 mol) was slowly added at room temperature over 60 min. After stirring for 16 h at the same temperature, the resulting precipitates were collected by filtration with a glass filter in a glovebox, and the white solid was washed with an excess amount of hexane for twice. Then, the white solid was dissolved in Et_2O, and upon slow immersion into cooling bath at −78 °C to obtain PhLi as colorless block crystals. The supernatant was quickly removed by cannulation. After a second recrystallization in the same manner, the crystals were dried under vacuum to give a white solid (9.35 g, 91%). ^1H NMR (500 MHz, THF-d_8, 25 °C): δ 7.93 (d, J = 6.4 Hz, 2H, *o*-H), 6.87 (t, J = 6.7 Hz, 2H, *m*-H), 6.77 (t, J = 7.2 Hz, 1H, *p*-H).

$[Li(thf)_n][RhPh_6\{Li(thf)\}_2]$ ($\mathbf{2_{Rh}}$). In a glovebox, PhLi (67.2 mg, 0.800 mmol) was dissolved in THF (1 mL) and slowly added to a suspension of $RhCl_3(tht)_3$ (47.4 mg, 0.100 mmol) in THF (3 mL) at room temperature. After stirring for 5 min at the same temperature, an excess amount of hexane (ca. 10 mL) was added to the resulting mixture. The supernatant was removed by decantation, and the resulting precipitates were dissolved in benzene (ca. 5 mL). The resulting mixture was filtered, and the solution was concentrated under vacuum to afford $\mathbf{2_{Rh}}$ as a beige solid (56.4 mg, 70%). Mp = 114 °C (dec.). IR (nujor): 2919, 2855, 1456, 1375 cm^{-1}. ^1H NMR (500 MHz, THF-d_8, 25 °C): δ 7.82 (d, J = 6.9 Hz, 12H, *o*-H), 6.55−6.54 (m, 18H, *m*- and *p*-H), 3.63−3.60 (m, thf), 1.79−1.76 (m, thf). ^{13}C NMR (126 MHz, CD_3CN, 25 °C): δ 162.3 (d, $^1J_{Rh-C}$ = 36.7 Hz, C_{ipso}), 141.3, 125.5(d, $^2J_{Rh-C}$ = 2.3 Hz, C_{ortho}), 120.9, 68.2 (thf), 26.2 (thf). ^7Li NMR (194 MHz, THF-d_8, −60 °C): δ 0.76, −0.58. Anal. Calcd for $C_{48}H_{54}O_3Li_3Rh$: C, 71.83; H, 6.78. Found: C, 71.85; H, 6.87. Single crystals of $\mathbf{3_{Rh}}$ suitable for X-ray crystallography were obtained by recrystallization of $\mathbf{2_{Rh}}$ from THF and pentane (vapor diffusion method) in the presence of 12-crown-4 at −25 °C under an Ar atmosphere.

$[Li(thf)_n][IrPh_6\{Li(thf)\}_2]$ ($\mathbf{2_{Ir}}$). In a glovebox, PhLi (135.7 mg, 1.61 mmol) was dissolved in THF (2 mL) and slowly added to a suspension of $IrCl_3(tht)_3$ (112.2 mg, 0.209 mmol) in THF (6 mL) at room temperature. After stirring for 5 min at the same temperature, an excess amount of hexane (ca. 20 mL) was added to the resulting mixture. The supernatant was removed by decantation, and the resulting precipitates were dissolved in benzene (ca. 10 mL). The resulting mixture was filtered, and the solution was concentrated under vacuum to afford $\mathbf{2_{Ir}}$ as a white solid (136.1 mg, 76%). Mp = 184 °C (dec.). IR (nujor): 2919, 2855, 1456, 1375 cm^{-1}. ^1H NMR (500 MHz, THF-d_8, 25 °C): δ 7.80 (dd, J = 3.1, 1.5 Hz, 12H, *o*-H), 6.55−6.48 (m, 18H, *m*- and *p*-H), 3.62−3.60 (m, thf), 1.79−1.76 (m, thf). ^{13}C NMR (126 MHz, THF-d_8, 25 °C): δ 164.8 (C_{ipso}), 144.3, 126.0, 119.0. ^7Li NMR (194 MHz, THF-d_8, −60 °C): δ 0.81 (2Li), −0.45 (1Li). Anal. Calcd for $C_{48}H_{54}O_3IrLi_3$: C, 64.63; H, 6.10. Found: C, 64.57; H, 5.97. Single crystals of $\mathbf{2_{Ir}}$ suitable for X-ray crystallography were obtained by recrystallization from THF. Single crystals of $\mathbf{3_{Ir}}$ suitable for X-ray crystallography were grown by recrystallization of complex $\mathbf{2_{Ir}}$ from THF and pentane (vapor diffusion method) in the presence of 12-crown-4 at −35 °C under an Ar atmosphere.

Reaction of $\mathbf{2_{Ir}}$ with CO_2 and CO. In a glovebox, $\mathbf{2_{Ir}}$ (11 mg, 12.5 μmol), mesitylene as an internal standard (5.0 μL), and THF-d_8 (0.65 mL) were charged into a NMR tube. After sealing it with a Teflon-lined screw cap, the NMR tube was brought out from the glovebox. The NMR tube was degassed by a freeze−thaw cycle (2 times) and refilled with CO or CO_2 gas (1 atm) via the screw cap. The reaction was monitored by ^1H NMR at room temperature.

DFT Calculation and FEFF Fitting Analysis of EXAFS. DFT calculations were carried out with the M06 functional[30] as implemented in the Gaussian 16 suite of programs.[31] Molecular structures were optimized at M06/Def2-SVP (and associated ECPs for Rh and Ir) level of theory using the molecular structure of $\mathbf{3_{Ir}}$ determined by X-ray crystallography as an initial geometry. The atomic coordinate of anionic part $[IrPh_6\{Li(thf)\}_2]^-$ extracted from the above DFT-calculated structure was used for the FEFF fitting. The FEFF fitting analysis of EXAFS spectra of $\mathbf{2_{Ir}}$ in THF using DFT-calculated atomic coordinate was carried out by IFEFFIT (revision 1.2.12)[32] embedded with Artemis.[33]

■ ASSOCIATED CONTENT

Supporting Information

The Supporting Information is available free of charge at https://pubs.acs.org/doi/10.1021/acs.organomet.1c00248.

Spectroscopic data, kinetics of $\mathbf{2_{Rh}}$ decomposition, X-ray crystallographic data, fitting analyses, and theoretical calculations (PDF)

Cartesian coordinates (XYZ)

Accession Codes

CCDC 2071930−2071932 contain the supplementary crystallographic data for this paper. These data can be obtained free of charge via www.ccdc.cam.ac.uk/data_request/cif, or by emailing data_request@ccdc.cam.ac.uk, or by contacting The Cambridge Crystallographic Data Centre, 12 Union Road, Cambridge CB2 1EZ, UK; fax: +44 1223 336033.

■ AUTHOR INFORMATION

Corresponding Authors

Takanori Iwasaki − *Department of Chemistry and Biotechnology, Graduate School of Engineering, The University of Tokyo, Tokyo 113-8656, Japan*; orcid.org/0000-0002-6663-3826; Email: iwasaki@chembio.t.u-tokyo.ac.jp

Kyoko Nozaki − *Department of Chemistry and Biotechnology, Graduate School of Engineering, The University of Tokyo, Tokyo 113-8656, Japan*; Email: nozaki@chembio.t.u-tokyo.ac.jp

Authors

Yuko Hirooka − *Department of Chemistry and Biotechnology, Graduate School of Engineering, The University of Tokyo, Tokyo 113-8656, Japan*

Hikaru Takaya − *Institute of Chemical Research, Kyoto University, Kyoto 611-0011, Japan; Department of Photo-Molecular Science, Institute for Molecular Science, Okazaki, Aichi 444-8585, Japan*; orcid.org/0000-0003-4688-7842

Tetsuo Honma − *Japan Synchrotron Radiation Research Institute (JASRI, SPring-8), Sayo, Hyogo 679-5198, Japan*

Complete contact information is available at:
https://pubs.acs.org/10.1021/acs.organomet.1c00248

Notes

The authors declare no competing financial interest.

■ ACKNOWLEDGMENTS

This work was partially supported by KAKENHI (JP16H06039) from JSPS. A part of this work was conducted at Advanced Characterization Nanotechnology Platform of the University of Tokyo (JPMXP09 A19UT0061 and A20UT0020), supported by Nanotechnology-Platform-Project by MEXT, Japan. The synchrotron XAS measurements were carried out at SPring-8 beamline of BL14B2 (2020A0950 and 2020A1879). The computations were carried out using the Research Center for Computational Science, Okazaki, Japan.

■ REFERENCES

(1) Selected examples of C−C bond formations using homoleptic organo transition metal species: (a) Cr: Nishikawa, T.; Kakiya, H.; Shinokubo, H.; Oshima, K. Novel [2 + 2 + 2]Annulation of 1,6-Diynes Mediated by Methallylchromate or Methallylmagnesium Chloride under $CrCl_3$ Catalysis. *J. Am. Chem. Soc.* **2001**, *123*, 4629−4630. (b) Hojo, M.; Sakuragi, R.; Okabe, S.; Hosomi, A. Allyl- and propargylchromium reagents generated by a chromium(III) ate-type reagent as a reductant and their reactions with electrophiles. *Chem. Commun.* **2001**, 357−358. (c) Hojo, M.; Sakata, K.; Ushioda, N.; Watanabe, T.; Nishikori, H.; Hosomi, A. Reductive Generation of Enolates Using a Chromium(III) Ate-Type Reagent as a Reductant and Reactions of the Enolates with Electrophiles. *Organometallics* **2001**, *20*, 5014−5016. (d) Mn: Valyaev, D. A.; Lavigne, G.; Lugan, N. Manganese organometallic compounds in homogeneous catalysis: Past, present, and prospects. *Coord. Chem. Rev.* **2016**, *308*, 191−235. (e) Uzelac, M.; Mastropierro, P.; de Tullio, M.; Borilovic, I.; Tarrés, M.; Kennedy, A. R.; Aromí, G.; Hevia, E. Tandem Mn−I Exchange and Homocoupling Processes Mediated by a Synergistically Operative Lithium Manganate. *Angew. Chem., Int. Ed.* **2021**, *60*, 3247−3253. (f) Co: Kauffmann, T.; Hopp, G.; Laarmann, B.; Stegemann, D.; Wingbermühle, D. Selektive Kohlenstoff-Kohlenstoff-Verknüpfungen mit Nucleophilen Thermolabilen Methylcobalt-reagenzien. *Tetrahedron Lett.* **1990**, *31*, 511−514. (g) Ohmiya, H.; Yorimitsu, H.; Oshima, K. Regio- and Stereoselective Approach to 1,2-Di- and 1,1,2-Trisilylethenes by Cobalt-Mediated Reaction of Silyl-Substituted Dibromomethanes with Silylmethylmagnesium Reagents. *Angew. Chem., Int. Ed.* **2005**, *44*, 3488−3490. (h) Cu: Lipshutz, B. H.; Wilhelm, R. S.; Kozlowski, J. A. The Chemistry of Higher Order Organocuprates. *Tetrahedron* **1984**, *40*, 5005−5038.

(2) (a) Roessler, B.; Pfennig, V.; Seppelt, K. Trigonal-Prismatic versus Octahedral Molecular Structures in $[(CH_3)_nMX_{6-n}]$ Compounds. *Chem. - Eur. J.* **2001**, *7*, 3652−3656. (b) Kaupp, M. Non-VSEPR" Structures and Bonding in d^0 Systems. *Angew. Chem., Int. Ed.* **2001**, *40*, 3534−3565. (c) Seppelt, K. Nonoctahedral Structures. *Acc. Chem. Res.* **2003**, *36*, 147−153.

(3) For d^0 metals, see (a) Morse, P. M.; Girolami, G. S. Are d^0 ML$_6$ Complexes Always Octahedral? The X-ray Structure of Trigonal-Prismatic $[Li(tmed)]_2[ZrMe_6]$. *J. Am. Chem. Soc.* **1989**, *111*, 4114−4116. (b) Kleinhenz, S.; Pfennig, V.; Seppelt, K. Preparation and Structures of $[W(CH_3)_6]$, $[Re(CH_3)_6]$, $[Nb(CH_3)_6]^-$, and $[Ta(CH_3)_6]^-$. *Chem. - Eur. J.* **1998**, *4*, 1687−1691. For d^3 metals, see (c) Morris, R. J.; Girolami, G. S. Permethyl Manganates. Synthesis and Characterization of Divalent $[MnMe_4{}^{2-}]$, Trivalent $[MnMe_5{}^{2-}]$, and Tetravalent $[MnMe_6{}^{2-}]$. *J. Am. Chem. Soc.* **1988**, *110*, 6245−6246. (d) Morris, R. J.; Girolami, G. S. High-Valent Organomanganese Chemistry. 1. Synthesis and Characterization of Manganese(III) and -(IV) Alkyls. *Organometallics* **1991**, *10*, 792−799. For d^6 metals, see (e) Hay-Motherwell, R. S.; Wilkinson, G.; Hussain, B.; Hursthouse, M. B. Homoleptic Methyl Compounds of Rhodium and Iridium(III). X-Ray Crystal Structures of Tetramethylethylenediamine Lithium Hexamethyl-rhodate(III) and -iridate(III). *J. Chem. Soc., Chem. Commun.* **1989**, 1436−1437. (f) Hay-Motherwell, R. S.; Wilkinson, G.; Hussain-Bates, B.; Hursthouse, M. B. Synthesis and Reactions of Tris(tetramethylethylenediaminelithium)-hexamethylmetallates of Rhodium, Iridium and Ruthenium(III) and of Hexakis(heopentyl)(μ-oxo)dirhodium(IV). X-Ray Crystal Structures of *fac*-$RhMe_3(CO)(Me_2NCH_2CH_2NMe_2)$, *fac*-$RhMe_3(C_4H_8S)(Me_2NCH_2CH_2NMe_2)$, *fac*-$RhMe_3(PMe_3)_3$ and $[(Me_3CCH_2)_3Rh]_2O$. *Polyhedron* **1990**, *9*, 2071−2080. (g) Rice, G. W.; Tobias, R. S. Pentamethyl- and Hexamethyl-platinate(IV). *J. Chem. Soc., Chem. Commun.* **1975**, 994−995. (h) Rice, G. W.; Tobias, R. S. Synthesis of Hexamethyl- and Pentamethylplatinate(IV) and Tetramethyl- and Trimethylplatinate(II) Complexes. Spectroscopic Studies of Organoplatinum Complexes. *J. Am. Chem. Soc.* **1977**, *99*, 2141−2149. (i) Creaser, C. S.; Creighton, J. A. A Simplified Synthesis of the Hexamethylplatinate(IV) Ion. *J. Organomet. Chem.* **1978**, *157*, 243−245.

(4) For a review, see (a) Buschbeck, R.; Low, P. J.; Lang, H. Homoleptic transition metal acetylides. *Coord. Chem. Rev.* **2011**, *255*, 241−272. For d^0 metals, see (b) Vaid, T. P.; Veige, A. S.; Lobkovsky, E. B.; Glassey, W. V.; Wolczanski, P. T.; Liable-Sands, L. M.; Rheingold, A. L.; Cundari, T. R. Structural Dichotomy in Six-Coordinate d^0 Complexes: Trigonal Prismatic $({}^tBu_3SiCC)_6Ta^-$ and Octahedral $({}^tBu_3SiCC)_6M^{2-}$ (M = Zr, Hf). *J. Am. Chem. Soc.* **1998**, *120*, 10067−10079. For d^3−d^7 metals, see (c) Nast, R.; Lewinsky, H. Alkinyloverbindungen von Übergangsmetallen. IV. Alkinylokomplexe von Kobalt(II) und Kobalt(III). *Z. Anorg. Allg. Chem.* **1955**, *282*, 210−216. (d) Nast, R.; Sirtl, E. Hexaalkinylokomplexe von Chrom(III). *Chem. Ber.* **1955**, *88*, 1723−1726. (e) Nast, R.; Urban, F. Alkinylokomplexe von Eisen(II) und Eisen(III). *Z. Anorg. Allg. Chem.* **1956**, *287*, 17−23. (f) Nast, R.; Griesshammer, H. Alkinylokomplexe von Mangan(II). *Chem. Ber.* **1957**, *90*, 1315−1320. (g) Nast, R.; Fock, K. Hexaalkinylcobaltate(II). *Chem. Ber.* **1976**, *109*, 455−458. (h) Rojas, E.; Santos, A.; Moreno, V.; Del Pino, C. Cyclohexylethynyl Complexes of Co^{II} and Fe^{II}. *J. Organomet. Chem.* **1979**, *181*, 365−373. (i) Berben, L. A.; Long, J. R. Homoleptic Trimethylsilylacetylide Complexes of Chromium(III), Iron(II), and Cobalt(III): Syntheses, Structures, and Ligand Field Parameters. *Inorg. Chem.* **2005**, *44*, 8459−8468.

(5) El-Kurdi, S.; Seppelt, K. Homoleptic Organometallic Anions of Ti, Zr, Hf, and Nb. *Chem. - Eur. J.* **2011**, *17*, 3956−3962.

(6) Kleinhenz, S.; Schubert, M.; Seppelt, K. Preparation and Structures of Hexaphenyl- and Hexatolyltantalates(V). *Chem. Ber.* **1997**, *130*, 903−906.

(7) Olmstead, M. M.; Power, P. P.; Shoner, S. C. Isolation and X-ray Crystal Structures of the Homoleptic, σ-Bonded, Transition-Metal Aryl Complexes $[(LiEt_2O)_4VPh_6]$ and $[(LiEt_2O)_3CrPh_6]$. *Organometallics* **1988**, *7*, 1380−1385.

(8) For $Li^+{}_2[HfPh_6]^{2-}$, the structure with two solvated Li cations and the structure with one solvated and one contacted Li cations have been determined by X-ray crystallography. See ref 5.

(9) Harrison-Marchand, A.; Mongin, F. Mixed AggregAte (MAA): A Single Concept for All Dipolar Organometallic Aggregates. 1. Structural Data. *Chem. Rev.* **2013**, *113*, 7470−7562.

(10) (a) Gschwind, R. M. Organocuprates and Diamagnetic Copper Complexes: Structures and NMR Spectroscopic Structure Elucidation in Solution. *Chem. Rev.* **2008**, *108*, 3029−3053. (b) Yoshikai, N.; Nakamura, E. Mechanisms of Nucleophilic Organocopper(I) Reactions. *Chem. Rev.* **2012**, *112*, 2339−2372.

(11) After 60 min, ^1H NMR showed only biphenyl in aromatic region, suggesting the formation of paramagnetic species bearing Ph groups.

(12) (a) Iwasaki, T.; Min, X.; Fukuoka, A.; Kuniyasu, H.; Kambe, N. Nickel-Catalyzed Dimerization and Alkylarylation of 1,3-Dienes with Alkyl Fluorides and Aryl Grignard Reagents. *Angew. Chem., Int. Ed.*

2016, *55*, 5550−5554. (b) Iwasaki, T.; Fukuoka, A.; Min, X.; Yokoyama, W.; Kuniyasu, H.; Kambe, N. Multicomponent Coupling Reaction of Perfuoroarenes with 1,3-Butadiene and Aryl Grignard Reagents Promoted by an Anionic Ni(II) Complex. *Org. Lett.* **2016**, *18*, 4868−4871. (c) Iwasaki, T.; Fukuoka, A.; Yokoyama, W.; Min, X.; Hisaki, I.; Yang, T.; Ehara, M.; Kuniyasu, H.; Kambe, N. Nickel-catalyzed coupling reaction of alkyl halides with aryl Grignard reagents in the presence of 1,3-butadiene: mechanistic studies of four-component coupling and competing cross-coupling reactions. *Chem. Sci.* **2018**, *9*, 2195−2211.

(13) Iwasaki, T.; Miyata, Y.; Akimoto, R.; Fujii, Y.; Kuniyasu, H.; Kambe, N. Diarylrhodates as Promising Active Catalysts for the Arylation of Vinyl Ethers with Grignard Reagents. *J. Am. Chem. Soc.* **2014**, *136*, 9260−9263.

(14) García-Monforte, M. A.; Alonso, P. J.; Forniés, J.; Menjón, B. New advances in homoleptic organotransition-metal compounds: The case of perhalophenyl ligands. *Dalton Trans.* **2007**, 3347−3359.

(15) García, M. P.; Oro, L. A.; Lahoz, F. J. Novel Anionic Aryl Complexes of Rh^{III}: $[Rh(C_6F_5)_5]^{2-}$ and $[Rh(C_6F_5)_4(CO)_2]^-$. *Angew. Chem., Int. Ed. Engl.* **1988**, *27*, 1700−1702.

(16) (a) Garcia, M. P.; Jimenez, M. V.; Cuesta, A.; Siurana, C.; Oro, L. A.; Lahoz, F. J.; Lopez, J. A.; Catalan, M. P.; Tiripicchio, A.; Lanfranchi, M. Synthesis and Reactivity of Mononuclear (Pentachlorophenyl)rhodium(II) Complexes. Structural Relevance of Rhodium-*o*-Chlorine Secondary Bonding. *Organometallics* **1997**, *16*, 1026−1036. Ir analog: (b) García, P. M.; Jiménez, M. V.; Oro, L. A.; Lahoz, F. J.; Tiripicchio, M. C.; Tiripicchio, A. A Homoleptic Mononuclear Iridium(II) Organometallic Complex: Synthesis and X-ray Structure of $[Ir(C_6Cl_5)_4]^{2-}$. *Organometallics* **1993**, *12*, 4660−4663.

(17) García-Monforte, M. A.; Ara, I.; Martín, A.; Menjón, B.; Tomás, M.; Alonso, P. J.; Arauzo, A. B.; Martínez, J. I.; Rillo, C. Homoleptic Organocobalt(III) Compounds with Intermediate Spin. *Inorg. Chem.* **2014**, *53*, 12384−12395.

(18) (a) Fürstner, A.; Martin, R.; Krause, H.; Seidel, G.; Goddard, R.; Lehmann, C. W. Preparation, Structure, and Reactivity of Nonstabilized Organoiron Compounds. Implications for Iron-Catalyzed Cross Coupling Reactions. *J. Am. Chem. Soc.* **2008**, *130*, 8773−8787. (b) Carpenter, S. H.; Baker, T. M.; Muñoz, S. B., III; Brennessel, W. W.; Neidig, M. L. Multinuclear iron−phenyl species in reactions of simple iron salts with PhMgBr: identification of $Fe_4(\mu\text{-}Ph)_6(THF)_4$ as a key reactive species for cross-coupling catalysis. *Chem. Sci.* **2018**, *9*, 7931−7939. For triarylferrate(II): (c) Bedford, R. B.; Brenner, P. B.; Carter, E.; Cogswell, P. M.; Haddow, M. F.; Harvey, J. N.; Murphy, D. M.; Nunn, J.; Woodall, C. H. TMEDA in Iron-Catalyzed Kumada Coupling: Amine Adduct versus Homoleptic "ate" Complex Formation. *Angew. Chem., Int. Ed.* **2014**, *53*, 1804−1808.

(19) (a) Fürstner, A.; Krause, H.; Lehmann, C. W. Unusual Structure and Reactivity of a Homoleptic "Super-Ate" Complex of Iron: Implications for Grignard Additions, Cross-Coupling Reactions, and the Kharasch Deconjugation. *Angew. Chem., Int. Ed.* **2006**, *45*, 440−444. (b) Carpenter, S. H.; Brennessel, W. W.; Neidig, M. L. Isolation and Characterization of a Homoleptic Tetramethylcobalt(III) Distorted Square-Planar Complex. *Organometallics* **2019**, *38*, 3486−3489.

(20) Iwasaki, T.; Akaiwa, T.; Hirooka, Y.; Pal, S.; Nozaki, K.; Kambe, N. Synthesis of and Structural Insights into Contact Ion Pair and Solvent-Separated Ion Pair Diphenyliridate Complexes. *Organometallics* **2020**, *39*, 3077−3081.

(21) For the benzene−Li^+ interaction, donor−acceptor energy *E* was calculated to be 4.12 kcal/mol; see Khanmohammadi, A.; Raissi, H.; Mollania, F.; Hokmabadi, L. Molecular structure and bonding character of mono and divalent metal cations (Li^+, Na^+, K^+, Be^{2+}, Mg^{2+}, and Ca^{2+}) with substituted benzene derivatives: AIM, NBO, and NMR analyses. *Struct. Chem.* **2014**, *25*, 1327−1342.

(22) The C(*ipso*)−C(*ortho*) bonds in $\mathbf{3_{Ir}}$ were elongated to 1.420 Å on average (average of C(*ortho*)−C(*meta*) and C(*meta*)−C(*para*) was 1.398 and 1.390 Å, respectively) probably due to the cation−π interaction.

(23) Among homoleptic hexaarylmetal complexes, attempts to measure ^7Li NMR have only been reported for $[VPh_6]^{4-}$. In the literature, however, it is only mentioned that a broad signal was observed, and the details are not available. See ref 7.

(24) ^7Li NMR of $LiBF_4$ in THF exhibited a signal at −0.88 ppm.

(25) Li NMR analyses of a lithium cuprate suggested that Li cation was solvated in THF but keeps a CIP structure in Et_2O. (a) Gschwind, R. M.; Rajamohanan, P. R.; John, M.; Boche, G. Direct insight into the ion pair equilibria of lithium organocuprates by ^1H, ^6Li HOESY experiments. *Organometallics* **2000**, *19*, 2868−2873. (b) John, M.; Auel, C.; Behrens, C.; Marsch, M.; Harms, K.; Bosold, F.; Gschwind, R. M.; Rajamohanan, P. R.; Boche, G. The Relation between Ion Pair Structure and Reactivities of Lithium Cuprates. *Chem. - Eur. J.* **2000**, *6*, 3060−3068.

(26) Sazonov, P. K.; Beletskaya, I. P. Carbonylmetallates—A Special Family of Nucleophiles in Aromatic and Vinylic Substitution Reactions. *Chem. - Eur. J.* **2016**, *22*, 3644−3653.

(27) Pangborn, A. B.; Giardello, M. A.; Grubbs, R. H.; Rosen, R. K.; Timmers, F. J. Safe and Convenient Procedure for Solvent Purification. *Organometallics* **1996**, *15*, 1518−1520.

(28) John, K. D.; Salazar, K. V.; Scott, B. L.; Baker, R. T.; Sattelberger, A. P. Comparison of the Reactivity of $M(allyl)_3$ (M = Rh, Ir) with Donor Ligands. *Organometallics* **2001**, *20*, 296−304.

(29) Schlosser, M.; Ladenberger, V. Notiz Über die darstellung reiner lithiumaryle. *J. Organomet. Chem.* **1967**, *8*, 193−197.

(30) Zhao, Y.; Truhlar, D. G. The M06 suite of density functionals for main group thermochemistry, thermochemical kinetics, non-covalent interactions, excited states, and transition elements: two new functionals and systematic testing of four M06-class functionals and 12 other functionals. *Theor. Chem. Acc.* **2008**, *120*, 215−241.

(31) Frisch, M. J.; Trucks, G. W.; Schlegel, H. B.; Scuseria, G. E.; Robb, M. A.; Cheeseman, J. R.; Scalmani, G.; Barone, V.; Petersson, G. A.; Nakatsuji, H.; Li, X.; Caricato, M.; Marenich, A. V.; Bloino, J.; Janesko, B. G.; Gomperts, R.; Mennucci, B.; Hratchian, H. P.; Ortiz, J. V.; Izmaylov, A. F.; Sonnenberg, J. L.; Williams-Young, D.; Ding, F.; Lipparini, F.; Egidi, F.; Goings, J.; Peng, B.; Petrone, A.; Henderson, T.; Ranasinghe, D.; Zakrzewski, V. G.; Gao, J.; Rega, N.; Zheng, G.; Liang, W.; Hada, M.; Ehara, M.; Toyota, K.; Fukuda, R.; Hasegawa, J.; Ishida, M.; Nakajima, T.; Honda, Y.; Kitao, O.; Nakai, H.; Vreven, T.; Throssell, K.; Montgomery, J. A., Jr.; Peralta, J. E.; Ogliaro, F.; Bearpark, M.; Heyd, J. J.; Brothers, E. N.; Kudin, K. N.; Staroverov, V. N.; Kobayashi, R.; Normand, J.; Raghavachari, K.; Rendell, A.; Burant, J. C.; Iyengar, S. S.; Tomasi, J.; Cossi, M.; Millam, J. M.; Klene, M.; Adamo, C.; Cammi, R.; Ochterski, J. W.; Martin, R. L.; Morokuma, K.; Farkas, O.; Foresman, J. B.; Fox, D. J. *Gaussian 16*, revision C.01; Gaussian, Inc.: Wallingford CT, 2016.

(32) Marenich, A. V.; Cramer, C. J.; Truhlar, D. G. Universal Solvation Model Based on Solute Electron Density and on a Continuum Model of the Solvent Defined by the Bulk Dielectric Constant and Atomic Surface Tensions. *J. Phys. Chem. B* **2009**, *113*, 6378−6396.

(33) (a) Newville, M. IFEFFIT: interactive XAFS analysis and FEFF fitting. *J. Synchrotron Radiat.* **2001**, *8*, 322−324. (b) Ravel, B.; Newville, M. ATHENA, ARTEMIS, HEPHAESTUS: data analysis for X-ray absorption spectroscopy using IFEFFIT. *J. Synchrotron Radiat.* **2005**, *12*, 537−541.